Supporting Information

Kinetic Analysis of Interaction of BRCA1 Tandem Breast Cancer C-Terminal Domains with Phosphorylated Peptides Reveals Two Binding Conformations

Yves Nominé, Maria Victoria Botuyan, Zeljko Bajzer, Whyte G. Owen, Ariel J. Caride, Emeric Wasielewski, and Georges Mer

Department of Biochemistry and Molecular Biology

Mayo Clinic College of Medicine

200 First Street S.W.

Rochester, Minnesota 55905 USA

Surface plasmon resonance

Biosensor surface preparation. Two types of biosensor surfaces were generated by using either streptavidin pre-coated sensor chips (SA sensor chip, BIAcore/GE Healthcare Bio-Sciences Corp., Piscataway, NJ) or shorter dextran layer chips (CM3 sensor chip, BIAcore/GE Healthcare Bio-Sciences Corp., Piscataway, NJ) where neutravidin was manually immobilized by an amine coupling procedure. Activation of the carboxymethylated dextran-coated surface of the CM3 chip was carried out by mixing equal volumes of 100 mM N-hydroxysuccinimide and 400 mM N-ethyl-N'-(dimethylaminopropyl)carbodiimide (made fresh with ultrapure water just before use) and injecting the mixture onto the chip at a flow rate of 5 µl min^{-1} for 7 min. The neutravidin (Pierce, Rockford, IL) to be coupled was first dissolved in 10 mM sodium acetate, pH 4.5, and then manually injected over the activated surface to immobilize about 700 RU of neutravidin. Unreacted sites were capped by injecting 1 M ethanolamine, pH 8.5, for 7 min. Biotin-labeled peptides (BACH1-P, BACH1-NP, CtIP-P and BACH1-P mutants) were immobilized on SA and CM3 chips by injection onto the chips at a concentration of 0.01 µg ml^{-1} and a flow rate of 80 µl min^{-1} for 5 to 10 min. This procedure keeps the binding capacity (achieved with 20 to 40 RU of biotinylated peptides) of the surface low, minimizing steric hindrance, mass transportation and crowding effects. Coupling with low amounts of neutravidin and biotinylated peptide

helped produced homogeneous surfaces. Reference surfaces without ligand were included on the chips to serve as controls for nonspecific binding and refractive index changes.

Improving the quality of SPR data. Deviation from the Langmuir model may arise from non-optimized experimental conditions and could result in the following artifacts: 1) parking problem or masking of potential ligand binding sites by previously formed complexes; 2) heterogeneity of coupled ligand; 3) rebinding of dissociated analyte; 4) mass transport limitation that occurs when transportation kinetics is slower than binding kinetics; or 5) nonspecific binding between ligand and analyte. We performed numerous controls to figure out which of these artifacts might be influencing the sensorgrams. We also carried out corrective experiments when an artifact was suspected.

1) We assumed that the parking problem was absent because of the low amount of ligand coupled to the matrix.

2) Any artifact related to heterogeneity of the coupled ligand was minimized by using an oriented ligand surface, and low amounts of highly purified biotinylated peptides and neutravidin for coupling. We tested that biotin tags to either C- or N-terminus of the peptide do not alter the sensorgrams.

3) A slight decrease in the dissociation rate with increasing analyte flow rate could indicate rebinding of dissociated analyte. We suppressed this artifact by injecting free non-biotinylated and phosphorylated BACH1 peptide into the BIAcore instrument for 5 min during the dissociation phase (*1-3*). We determined and used the optimal

concentration of this peptide above for which the dissociation signal was not affected further. The peptide concentration was 20 μM.

4) To assess contribution from mass transportation, we injected at varying flow rates (5, 15 and 75 μl min^{-1}) 2 μM of BRCA1-BRCT on surfaces with 20 and 100 RU peptide immobilization levels. Since we did not observe marked differences in the normalized association time course plots, the mass transportation effect could be considered negligible. This was confirmed by using the "two-compartments" mass transfer model (*4, 5*) and simulating a reaction time course for a 40 RU immobilization level and $k_a = 10^6$ $M^{-1}s^{-1}$ (association rate for the fastest reaction). This model did not predict major mass transfer distortion of the data except in the first few seconds of the association and dissociation phases.

5) Possible nonspecific binding of BRCA1-BRCT to non-biotinylated BACH1-P was minimized by using low level of avidin. Instead of using a streptavidin pre-coated chip (SA sensor chip, BIAcore), we manually immobilized neutravidin onto a CM3 chip at a level of 700 RU, which is equivalent to only $1/10^{th}$ to $1/5^{th}$ of the level used in SA chips.

In summary, to minimize experimental artifacts described above, the SPR experiments were performed at high flow rate (50 μl min^{-1}), low amount of immobilized ligand (20 RU on CM3 chip), and with injection of 20 μM of free non-biotinylated BACH1-P during the dissociation phase.

Processing of SPR data. Data were processed with BIAevaluation 4.1 (Biacore AB, St. Albans, Hertfordshire, England). Sensorgrams were corrected for bulk refractive index changes, matrix effects, injection noise, and nonspecific binding, by subtracting the

sensorgrams corresponding to BRCA1-BRCT injection to the reference cell and buffer injection to BACH1-P surface. This procedure referred to as "double referencing" accounts for any buffer effect on the peptide, and any protein effect on the matrix and improves significantly the quality of data (*6*).

Linearization of SPR data. For the association phase, replotting the derivative of the signal *R* against *R* should give a straight line according to equation s1 (*3*):

$$\frac{dR}{dt} = k_{on}CR_{\max} - \left(k_{on}C + k_{off}\right)R \qquad \text{(s1)}$$

The observable rate k_{obs} is derived from the slop of the linear representation above:

$$slope = k_{obs} = -k_{on}C - k_{off} \qquad \text{(s2)}$$

Theoretically, k_{obs} is linearly dependent on the concentration of BRCA1-BRCT or *C*, with the rate constant k_{on} being the slope of the plot of k_{obs} versus *C*.

For the dissociation phase, assuming that the signal follows a single exponential decay function, the change of *R* (or *dR/dt*) should be proportional to *R*, i.e., $dR/dt = -k_{off} R$. Integration of this equation yields the linear equation s3 where the logarithm of *R* is directly proportional to time:

$$\ln R = \ln R_0 - k_{off}t \qquad \text{(s3)}$$

This expression shows that during the dissociation phase, *R* should be independent of the analyte or BRCA1-BRCT concentration.

Fluorescence anisotropy study

Fluorescence anisotropy titrations were performed on 4 μM of dansyl-BACH1-P (dBACH1-P) with 0 to 7.5 μM of BRCA1-BRCT. The excitation and emission wavelengths were 332 and 580 nm with slits widths of 5 and 10 nm, respectively. The photomultiplier voltage used was 800 V with an integration time of 5 sec. Anisotropy data were fitted with ORIGIN 7.0 (MicroCal, LLC, Northampton, MA) following equation s5 which describes the ratio of bound to free analyte in equilibrium:

$$Signal = \left((A_0 + B_0 + K_d) - \sqrt{(A_0 + B_0 + K_d)^2 - 4A_0B_0} \right) / (2A_0) \qquad \text{(s4)}$$

where A_0 and B_0 are the total concentrations of BRCA1-BRCT protein (analyte) and BACH1 phosphopeptide (ligand), respectively. Notice that this equation does not imply any approximation with respect to the protein or peptide concentration.

Errors on fitted parameters

Errors on fitted parameters were estimated by Monte Carlo simulation (*7*). The binding curves were simulated based on the best-fit model randomly altered by addition of Gaussian noise determined from the standard deviations of experimental data. The

standard deviations of the parameters were calculated from the distributions obtained after fitting 50 complete sets of simulated curves.

Model selection criteria

We used the modified Akaike selection criterion (MSC) defined by equation s5 (Scientist Handbook, 1995, p467, MicroMath Scientific Software, UT, USA) (*8*); Bayesian selection criterion (BIC) defined by equation s6 (*10, 11, 12*); and Hannan-Quinn information criterion given by equation s7 (*12, 13*):

$$MSC = \ln\left(\Phi \Big/ \chi^2\right) + 2\frac{m}{n} \tag{s5}$$

$$BIC = \left(\chi^2 + m\ln n\right)\Big/ n \tag{s6}$$

$$HQIC = \left(\chi^2 + 2m\ln(\ln n)\right)\Big/ n \tag{s7}$$

where $\chi^2 = \sum_{i=1}^{n}\left(y_i^e - y_i^t\right)^2 \Big/ \sigma_i^2$, $\Phi = \sum_{i=1}^{n}\left(y_i^e - \bar{y}\right)^2$ and $\bar{y} = \sum_{i=1}^{n}\frac{y_i^e}{n}$.

σ_i is the standard deviation of experimental data points, n is the number of experimental data points y_i^e, m is the number of free parameters in the model and y_i^t are the best fit values predicted by the model. The model with larger MSC and lower BIC and HQIC is chosen as the most appropriate description of the data.

The Zwanzig model selection criterion based on the comparison statistic T_{uv} (defined in equation s8) was used to compare models *u* and *v* (*9, 10*):

$$T_{uv} = \sqrt{\frac{n}{4}} \frac{Q_u - Q_v}{\sqrt{\frac{1}{n}\sum_{i=1}^{n} \omega_i^2 \sigma_i^2 \left(u_i - v_i\right)^2}} \qquad \text{(s8)}$$

where $Q_u = \frac{1}{n}\sum_{i=1}^{n} \omega_i \left(y_i^e - u_i\right)^2$ and $Q_v = \frac{1}{n}\sum_{i=1}^{n} \omega_i \left(y_i^e - v_i\right)^2$

ω_t are weighing factors and σ_t are standard deviations in data y_i^e. We set the weighting factors to be $\omega_i = \sigma_i^{-2}$. Such a choice is motivated by the maximum likelihood method. u_i and v_i are the best fit values predicted by models *u* and *v*, respectively. If $T_{uv} > 1.96$, model *v* is more appropriate than model *u* (with significant level $\alpha = 0.05$). If $|T_{uv}| \leq 1.96$, there is no significant difference between the two models. If $T_{uv} < -1.96$, model *u* is a better representation than model *v*.

References

1. Felder, S., Zhou, M., Hu, P., Urena, J., Ullrich, A., Chaudhuri, M., White, M., Shoelson, S. E., and Schlessinger, J. (1993) SH2 domains exhibit high-affinity binding to tyrosine-phosphorylated peptides yet also exhibit rapid dissociation and exchange, *Mol. Cell. Biol*. *13*, 1449-1455.

2. Glaser, R. W. (1993) Antigen-antibody binding and mass transport by convection and diffusion to a surface: a two-dimensional computer model of binding and dissociation kinetics, *Anal. Biochem. 213*, 152-161.

3. Hall, D. (2001) Use of optical biosensors for the study of mechanistically concerted surface adsorption processes, *Anal. Biochem. 288*, 109-125.

4. Schuck, P. (1996) Kinetics of ligand binding to receptor immobilized in a polymer matrix, as detected with an evanescent wave biosensor. I. A computer simulation of the influence of mass transport, *Biophys. J. 70*, 1230-1249.

5. Myszka, D., He, X., Dembo, M., Morton, T., and Goldstein, B. (1998) Extending the range of rate constants available from BIACORE: interpreting mass transport-influenced binding data, *Biophys. J. 75*, 583-594.

6. Myszka, D. (1999) Improving biosensor analysis, *J. Mol. Recognit. 12*, 279-284.

7. Press W.H., Flannery B.P., Teukolsky S.A., and Vetterling W.T. (1992) Numerical Recipes, Cambridge Univ. Press, Cambridge.

8. Akaike, H. (1976) An information criterion (AIC), *Math. Sci. 14*, 5-9.

9. Zwanzig, S. (1980) The choice of approximative models in nonlinear regression, *Statistics 11*, 23-47.

10. Buckwitz, D., and Holzhutter, H.-G. (1990) A new method to discriminate between enzyme-kinetic models, *Math. Applic. 20*, 117-126.

11. Schwarz, G. (1978) Estimating the dimension of a model, *Ann. Stat. 6*, 461-464.

12. Davidian, M., and Gallant, A. R. (1993) The nonlinear mixed effects model with a smooth random effects density, *Biometrika 80*, 475-488.

13. Hannan, E. J. (1987) Rational transfer function approximation, *Statist. Sci. 2*, 1029-1054.

Supplementary figure

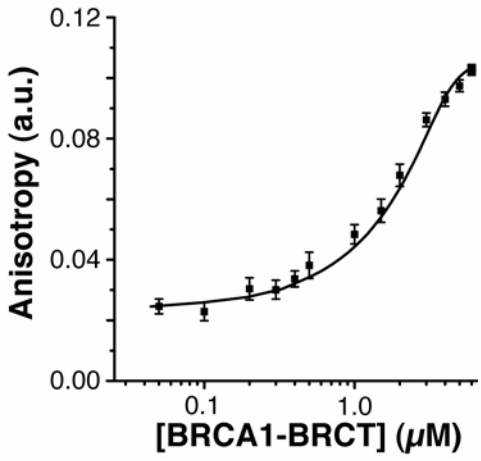

Figure S1: BACH1 phosphopeptide titration with BRCA1-BRCT monitored by fluorescence anisotropy. The concentration of dansylated BACH1 phosphopeptide was 4 μM. Excitation and emission wavelengths were 332 and 580 nm, respectively. The solid line represents the least squares fit of the data to a single-binding site model. The fit corresponds to an equilibrium dissociation constant of 0.18 ± 0.05 μM.

Supplementary Tables

Table S1. Proteins and peptides used in this study.

Name	Sequence
BRCA1-BRCT:	tandem BRCT domains of BRCA1 (1646-1859)
BRCA1-BRCT-ct	C-terminal BRCT domain of BRCA1 (1760-1859)
BACH1-P (985-997):	I S R S T pS P T F N K Q T
BACH1-NP (985-997):	I S R S T S P T F N K Q T
P/A BACH1-P (985-997**)**:	I S R S T pS A T F N K Q T
CtIP-P (321-333):	P T R V S pS P V F G A T S
CtIP-NP (321-333):	P T R V S S P V F G A T S
bBACH1-P (985-997):	biotin-6 aa linker-G S G S I S R S T pS P T F N K Q T
bBACH1-NP (985-997):	biotin-6 aa linker-G S G S I S R S T S P T F N K Q T
dBACH1-P (985-997):	dansyl-6 aa linker-G S G S I S R S T pS P T F N K Q T
bCtIP-P (322-333):	biotin-6 aa linker-G S G S T R V S pS P V F G A T S

BACH1 peptides are derived from the DNA repair helicase BACH1 protein. CtIP peptides are derived from the transcriptional co-repressor CtIP. pS indicates a phosphoserine.

Table S2. Temperature dependence of the thermodynamic parameters of the binding of BRCA1-BRCT to BACH1-P by ITC in 50 mM sodium phosphate, pH 7.5, 300 mM NaCl.

T (ºC)	*n*	K_d (μM)	ΔH^o (kcal M^{-1})	ΔG^o [a] (kcal M^1)	$-T\Delta S^o$ [b] (kcalM^{-1})
10.0	0.92 ± 0.04	0.10 ± 0.01	-11.1 ± 0.6	-9.07 ± 0.04	2.0 ± 0.6
12.7	1.00 ± 0.03	0.15 ± 0.01	-11.1 ± 0.3	-8.94 ± 0.03	2.1 ± 0.4
15.0	0.93 ± 0.02	0.18 ± 0.01	-12.1 ± 0.4	-8.89 ± 0.03	3.1 ± 0.5
17.5	0.95 ± 0.05	0.22 ± 0.02	-12.2 ± 0.7	-8.84 ± 0.05	3.3 ± 0.8
20.0	1.01 ± 0.04	0.31 ± 0.01	-13.0 ± 0.4	-8.73 ± 0.02	4.3 ± 0.5
22.5	0.96 ± 0.03	0.35 ± 0.01	-14.2 ± 0.4	-8.74 ± 0.02	5.6 ± 0.5
25.0	0.99 ± 0.03	0.44 ± 0.02	-14.8 ± 0.4	-8.65 ± 0.02	6.1 ± 0.6
25.0	0.95 ± 0.03	0.43 ± 0.02	-15.5 ± 0.2	-8.64 ± 0.02	6.5 ± 0.6
28.0	1.02 ± 0.05	0.58 ± 0.03	-15.4 ± 0.6	-8.59 ± 0.03	6.8 ± 0.8
30.0	0.95 ± 0.05	0.60 ± 0.02	-16.8 ± 0.4	-8.58 ± 0.02	8.4 ± 0.6
32.5	0.91 ± 0.04	0.81 ± 0.03	-17.8 ± 0.8	-8.52 ± 0.02	9.3 ± 0.9
35.0	0.92 ± 0.06	1.03 ± 0.05	-18.4 ± 1.1	-8.44 ± 0.03	10 ± 1
37.5	0.84 ± 0.06	1.49 ± 0.09	-19.4 ± 1.5	-8.28 ± 0.04	11 ± 2
40.0	0.81 ± 0.06	2.0 ± 0.1	-21 ± 2	-8.18 ± 0.05	13 ± 3
45.0	0.40 ± 0.09	3.2 ± 0.1	-26 ± 3	-7.99 ± 0.08	18 ± 5

[a] Calculated from $\Delta G^o = RT\ln(K_d)$.
[b] Calculated from $\Delta G^o = \Delta H^o - T\Delta S^o$.

Table S3. Temperature dependence of the steady-state analysis parameters of the binding of BRCA1-BRCT to 15 RU of immobilized bBACH1-P by SPR in 50 mM sodium phosphate, pH 7.5, 300 mM, 0.005% P20[a].

T (ºC)	R_{min} (RU)	R_{max} (RU)	K_d (μM)	Sig/R_{max}(%) [b]
10	-5 ± 2	144 ± 2	0.074 ± 0.008	93.8
15	-4 ± 2	155 ± 3	0.092 ± 0.01	104.2
20	-5 ± 3	158 ± 5	0.15 ± 0.02	107.7
25	-5 ± 2	152 ± 3	0.33 ± 0.04	99.6
25	-2 ± 5	147 ± 4	0.35 ± 0.06	101.5
30	-4 ± 2	160 ± 8	0.43 ± 0.06	93.8
35	-3 ± 4	120 ± 10	0.76 ± 0.15	88.5

[a] Steady-state parameters were obtained from data fitted to the Langmuir isotherm in terms of equation 2.
[b] Ratio of the steady-state binding signal R_{eq} obtained for the highest BRCA1-BRCT concentration with the R_{max} fitted value.